Rare Metal Materials and Engineering
Volume 48, Issue 1, January 2019
Available online at www.rmme.ac.cn

Science Press

Cite this article as: Rare Metal Materials and Engineering, 2019, 48(1): 0097-0103

ARTICLE

Microstructural Evolution and Continuous Cooling Transformation Diagram in Ti-1300 Alloy Under Continuous Cooling Condition

Wan Mingpan[1], Wen Xin[1], Ma Rui[1], Zhao Yongqing [2]

[1] Guizhou University, Guiyang 550025, China; *[2] Northwest Institute for Nonferrous Metal Research, Xi'an 710016, China*

Abstract: Microstructural evolution of Ti-1300 alloys was investigated using optical microscopy, scanning electron microscopy, transmission electron microscopy and electron backscatter diffraction during continuous cooling. Then, a continuous cooling transformation diagram was established using a dilatometer method, and the different kinds of β phase decomposition modes in the alloy under continuous cooling were investigated. Results show that the $\beta \rightarrow \alpha + \beta$ phase transformation and colony structures are observed for low cooling rates. When the cooling rate is from 0.3 °C/s to 1.5 °C/s, the $\beta \rightarrow \alpha + \beta + \beta_m$ phase transformation and needle-like structures are observed in the alloy. However, when the cooling rate exceeds 3 °C/s, the alloy is only composed of a single metastable β phase. Thus, a rate of 3 °C/s is considered as the critical cooling rate of the alloy under continuous cooling condition. The concentration gradient of molybdenum equivalent is considered as a driving force of α phase growth in the alloy. The microhardness of the alloy initially increases and then decreases with increasing of the cooling rate. When the cooling rate is 0.3 °C/s, the microhardness of the alloy reaches its maximum.

Key words: Ti-1300 alloy; microstructural evolution; transformation diagram; continuous cooling; microhardness

Metastable β titanium alloys provide an excellent balance of mechanical properties compared with other titanium alloys. Metastable β titanium alloys are widely applied in aerospace and automotive industries owing to their strength-to-density ratio and excellent stress corrosion resistance[1-5]. The alloys do not transform martensitically upon fast cooling from a single β-phase field[6]. This characteristic is attributed to the presence of a significant amount of β stabilizer elements, such as Mo, V, Fe, and Cr, in the metastable β alloys. Particularly, a significant advantage of metastable β alloys is their high strength and reasonable toughness as a result of uniform and fine dispersion α precipitation after solution treatment and aging [2]. The substantial influence of the microstructure on the properties of titanium alloys is widely understood. However, microstructural formation of the alloy during the heat treatment process is important. Cooling after solution treatment is one of the important processing steps for improving microstructural morphology and size to optimize the mechanical properties of titanium alloys. The microstructures of some common titanium alloys under continuous cooling conditions have been reported[7–10]. The transformation of the β phase into α, α", and α' phases under continuous cooling in $\alpha + \beta$ titanium alloys is well-known [11]. In metastable β alloys, the β phase may or may not be transformed into the α phase under continuous cooling from elevated temperatures to room temperature because the martensitic starting transformation temperature is below room temperature. Generally speaking, the β phase should preferably not be transformed under continuous cooling after solution treatment. Therefore, metastable β alloys possess obvious similarities to steels in terms of having a critical cooling rate under continuous cooling.

Received date: January 09, 2018
Foundation item: National Natural Science Foundation of China (51401058); Science and Technology Cooperative Foundation of Guizhou Province ([2015]7655); Youth Growth Project of Guizhou Education Department ([2016]122); Science and Technology Foundation of Guizhou Province ([2017]1023)
Corresponding author: Wan Mingpan, Ph. D., Associate Professor, College of Materials and Metallurgy, Guizhou University, Guiyang 550025, P. R. China, Tel: 0086-851-83627683, E-mail: mpwan@gzu.edu.cn

Continuous cooling transformation (CCT) diagrams can be used to describe the phase transformation of some metallic materials under continuous cooling. As for titanium alloys, according to the CCT diagram, reasonable cooling methods could be chosen to achieve desirable mechanical properties. However, only very few CCT diagrams have been developed for titanium alloys. Angelier built a CCT diagram of the β-CEZ alloy and analyzed its phase transformation mechanism by metallography and electrical resistivity [8]. S. Malinov studied the kinetics of the $\beta \rightarrow \alpha$ phase transformation and plotted a CCT curve of the Ti–6Al–4V titanium alloy using differential scanning calorimetry (DSC) [9]. S. K. Kim plotted a CCT curve of CP-Ti using a fully computer-controlled resistivity–temperature real-time measurement apparatus [10].

Dilatometry, however, was widely used as an experimental technique for studying various solid phase transformations[12-17]. In the present work, dilatometry was used to plot the CCT diagrams of the new metastable β titanium alloy (Ti-1300 alloy). The Ti-1300 alloy (Ti-5Al-4Mo-4V-4Cr-3Zr), which was developed by Northwest Institute for Nonferrous Metal Research in China, is a high strength and toughness titanium alloy that belongs to a six-component system[18]. Ti-1300 alloys present specific strength and toughness superiorities when compared to Ti-1023 alloys based on experiments[19]. Previous studies have focused on the mechanical properties, phase transformation and deformation behavior of the alloys[20-25]. The current study aimed to investigate the microstructural evolution and the CCT diagram of the Ti-1300 alloy under continuous cooling.

1 Experiment

Ti-1300 alloys were fabricated using a vacuum arc melting furnace by Northwest Institute for Nonferrous Metal Research in China. The ingots were re-melted for three times to ensure compositional homogeneity. The microstructure of the as-received rod at room temperature consisted of residual β phase and β transformation microstructure. Then the rolled-bar with 12 mm in diameter was obtained through rolling. Subsequently, the β-transus temperature of the Ti-1300 titanium alloy is about (830±5) °C, which was measured using the metallographic observation method. The cylindrical specimens with 4 mm in diameter and 25 mm in length were taken from the rolled bars using a wire-electrode cutting saw for continuous cooling tests at various cooling rates. Specimens were initially heated up to 850 °C and isothermally held for 40 min. The cooling tests were carried out on a DIL805A/D and a DIL 402 dilatometer under high purity Ar (99.999%) flow to prevent oxidation. The specimens were then cooled at various rates, including 0.01, 0.1, 0.3, 0.5, 1, 1.5, 2, 3, 4, and 5 °C/s. Furthermore, other samples, which were cooled to 690, 670, 650, 630, and 610 °C at a rate of 0.1 °C/s, can be used in observing the nucleation and growth mechanism of the $\beta \rightarrow \alpha + \beta$ phase transformation in the Ti-1300 alloy.

Metallographic specimens were prepared for observations by optical microscopy and scan electron microscopy by mechanical grinding, polishing, and etching with Kroll's reagent solution (20%HF+20%HNO_3+50%H_2O). The microstructural constituents were analyzed using a Leica DMI5000M and a SUPRA40. Thin-foil specimens were prepared for transmission electron microscopy analysis by ion polishing, and then these specimens were examined using a Tecnai G2 F20 at 200 kV. The chemical component was investigated by energy dispersive X-ray spectroscopy. Moreover, the electron backscattered diffraction (EBSD) analysis was performed on the SUPRA40 at specimens tilted at 70°.

2 Results and Discussion

2.1 Microstructural evolution

Fig.1 shows the room temperature microstructure of Ti-1300 alloys under continuous cooling at various cooling rates from the single β phase field at 850 °C. The room temperature microstructure clearly consists of α lamella and β phase between the α lamella under continuous cooling at 0.01 and 0.1 °C/s (Fig.1a and 1b). As shown in Fig.1, the observed differences in the microstructure of the specimens include morphology, size, arrangement, and volume fraction of α phase. The average thickness of each platelet-like α phase decreased in the microstructure when the cooling rate increased under the continuous cooling conditions. In addition, the α phase showed a basketweave morphology when the specimens were cooled at faster rates no more than 0.3 °C/s.

When Ti-1300 alloys were cooled at sufficiently low rates from the β phase field, such as 0.01 °C/s and 0.1 °C/s, a continuous α layer forming along prior β/β grain boundaries in the alloys is clearly observed. This typical α phase is called α_{GB} (Fig.1a). Furthermore, the lamellar α+β microstructure formed within prior coarse β grains and a prior β grain contained several α colonies. These typical α colonies are called Widmanstatten colonies (α_{WGB}) (Fig.1a). Each α platelet was separated within one α colony by the retained β phase. The residual metastable β phase appeared in the microstructure of the alloys when the cooling rates were faster than 0.3 °C/s (Fig.1c and 1d). Moreover, the volume fraction of the retained β phase increased in the Ti-1300 alloy when the cooling rate was increased under continuous cooling. The reason for these is that the Ti-1300 alloy contains a number of β stabilizer elements, such as Mo, V, and Cr. These alloy elements were able to stabilize β phase in the Ti-1300 alloy, and thus the β phase could not transform into other phases when accelerating the cooling process. Therefore, the $\beta \rightarrow \alpha+\beta$ phase transformation was gradu-

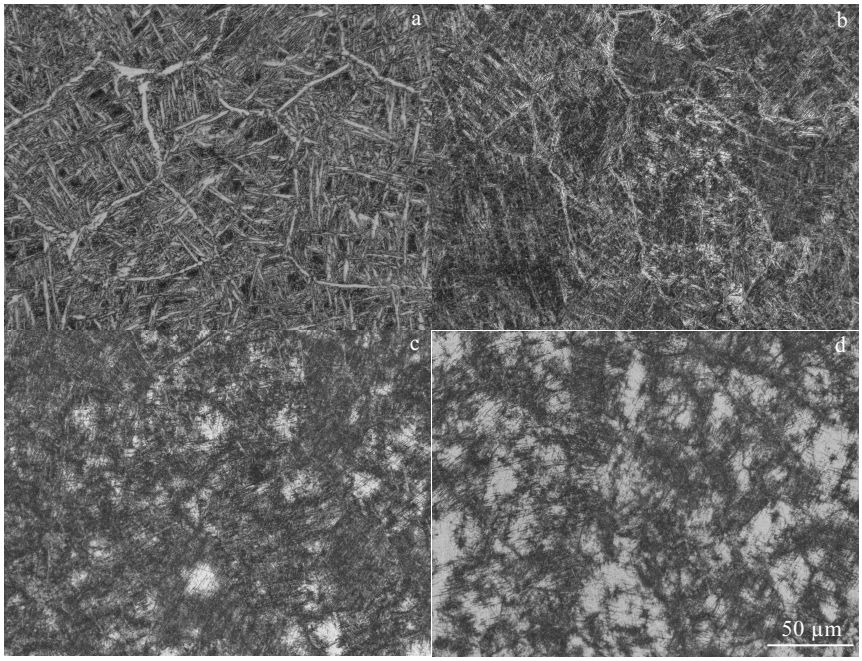

Fig.1 Microstructures of Ti-1300 alloy at various cooling rates: (a) 0.01 °C/s, (b) 0.1 °C/s, (c) 0.3 °C/s, and (d) 0.5 °C/s

ally suppressed when the alloys were cooled at rates faster than 0.3 °C/s. Moreover, a fine needle-like α phase formed only near β grain boundaries at a cooling rate from 0.5 °C/s to 2.5 °C/s. Therefore, the room temperature microstructure of the Ti-1300 alloy only contained a metastable β phase at cooling rates faster than 3 °C/s. Thus, 3 °C/s was considered as a critical cooling rate for Ti-1300 alloys under continuous cooling conditions.

Fig.2 shows TEM images of the Ti-1300 alloys continuously cooled at rates of 0.01 and 0.5 °C/s from the single β phase field at 850 °C. A coarse platelet-like microstructure was found in the Ti-1300 alloys continuously cooled at 0.01 °C/s (Fig.2a). However, the microstructure contained a needle-like α phase and retained β phase when the alloys were cooled at 0.5 °C/s. The maximum thickness of the α platelets in the alloy cooled at 0.01 °C/s reached approximately 2.6 μm, which is far greater than that of the alloy continuous cooled at 0.5 °C/s. Moreover, the α platelets in the α colonies of the alloy cooled at the same cooling rate had varying thicknesses. Previously formed α platelets were also likely to be coarser than later formed α platelets in the same β grain under continuous cooling (Fig.1a). The $\beta \rightarrow \alpha + \beta$ transformation in the titanium alloy is a typical diffusion continuous cooling process, and the degree of undercooling is formation under continuous cooling. The slower cooling rates decreases the nucleation driving force of the α phase. However, it is well known that temperature exert the most profound influence on the diffusion coefficients, and the diffusion abilities of atoms decrease with the increase of cooling rate. Thus, coarse lamellar $\alpha+\beta$ microstructures could be observed upon slower cooling from the single β phase field in the alloy. Moreover, the initially formed α platelets presented a coarse feature, but the later-formed α phases showed a needle-like feature. The time needed for α platelet growth was insufficient when the cooling rate was increased. Therefore, finer needle-like α phases could only be observed at faster cooling rates under continuous cooling.

2.2 Growth behavior of the α phase

In order to observe nucleation and growth of the α phase in Ti-1300 titanium alloys under continuous cooling, the specimens were continuously cooled to 690, 670, 650, 630, 610, and 590 °C at a rate of 0.1 °C/s from the single β phase field, and then rapidly cooled to room temperature at a cooling rate of 80 °C/s. Thereafter, the microstructural evolution of the $\beta \rightarrow \alpha+\beta$ transformation was traced using SEM and EBSD. Fig.3 shows the microstructures of Ti-1300 alloys cooled to different temperatures from the single β phase field. The EBSD orientation maps for Ti-1300 alloy quenched from 690 and 650°C are shown in the Fig.4. The volume fraction of α phase was found to increase with decreasing temperature. In addition, the initial formation of the α phase with different orientation at β/β grain boundaries under continuous cooling was clearly observed (Fig.4a). These observations can be attributed to the beneficial nature of β grain boundaries in the nucleation of the α phase because of their characteristics, which include constituent

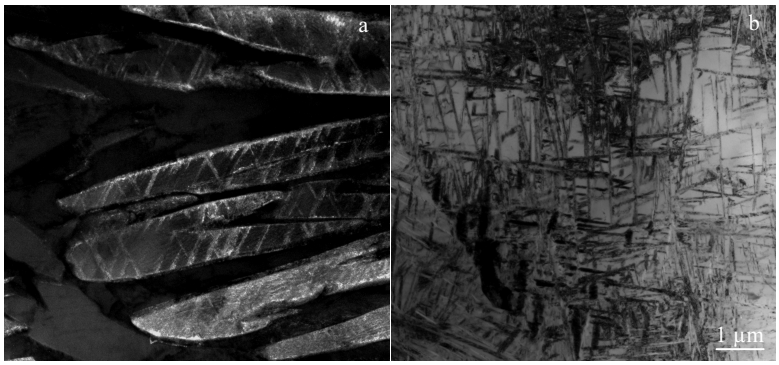

Fig.2 TEM micrographs of specimens cooled at a cooling rate of 0.01 °C/s (a) and 0.5 °C/s (b)

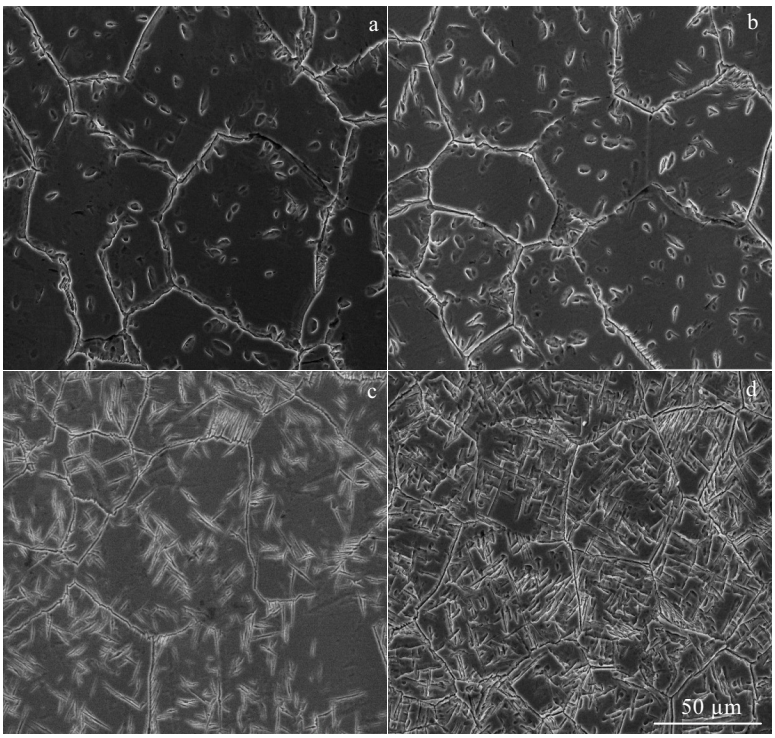

Fig.3 SEM images of Ti-1300 alloy quenched at different temperatures upon continuous cooling at a cooling rate of 0.1 °C/s: (a) 690 °C, (b) 670 °C, (c) 650 °C, and (d) 630 °C

fluctuation, structural fluctuation, and energy fluctuation[26]. However, few granular α phase also formed within the prior β grain of the alloy. Subsequently, the α phases that formed at β grain boundaries grew into a β grain along one favorable plane and direction with decreasing of temperature (Fig.3c and Fig.4b). This phenomenon is called variant selection, which is associated with the crystallographic parameters of the β/β grain boundaries [27]. Moreover, with decreasing temperature, the morphology of the α phase gradually evolved from granular to acicular, forming basket-weave structures.

Fig.5 shows molybdenum equivalent changes of the β phase near α/β boundaries of Ti-1300 alloys under continuous cooling at different temperatures from the single β phase field. A formula for molybdenum equivalency of alloying elements may be derived as follow[28]:

$$[Mo]_{eq.}=1.0(wt\%Mo)+0.67(wt\%V)+1.53(wt\%Mn)+0.44(wt\%W)+1.6(wt\%Cr)+0.28(wt\%Nb) \quad (1)$$

The molybdenum equivalent increased with decreasing of temperature under continuous cooling. The diffusion behavior of the atoms was demonstrated in the growth process of α phase.

Fig.6 schematically illustrates the chemical component changes that accompany the gradual growth of the α phase in the alloy under continuous cooling. For example, when the alloy having a composition of C_0 [Mo]eq. was cooled to a temperature (T) in Fig.6a, the concentration of β stabilizing elements of α and β phase near α/β boundaries was ex-

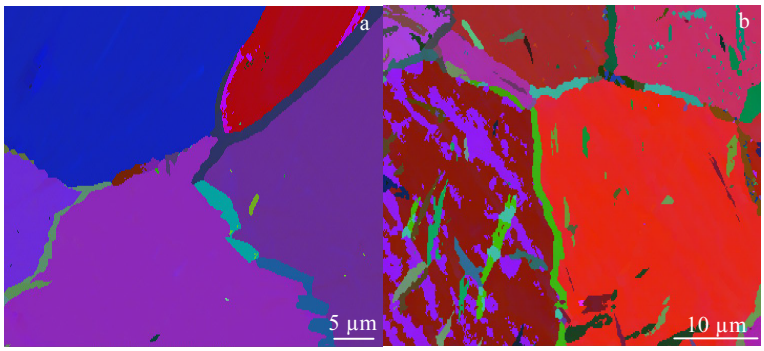

Fig.4 EBSD orientation maps for Ti-1300 alloy quenched from 690 °C (a) and 650 °C (b)

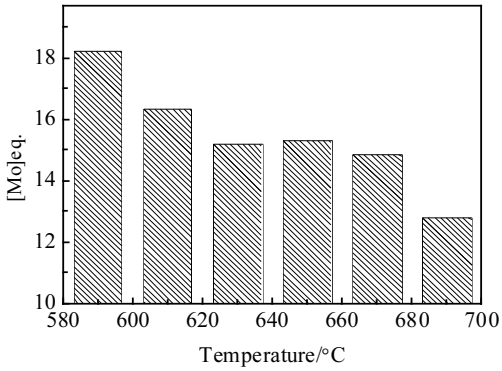

Fig.5 Molybdenum equivalent of β phase near α/β boundaries of Ti-1300 alloy after continuous cooling to different temperature after solution treatment

pressed as $C_{\alpha}^{\alpha/\beta}$ and $C_{\beta}^{\beta/\alpha}$ ($C_{\alpha}^{\alpha/\beta} < C_{\beta}^{\beta/\alpha}$), respectively. With decreasing temperature, the concentration gradient ($C_{\beta}^{\beta/\alpha} - C_0$) in the β phase was generated, and as a result more and more β stabilizing elements diffuse to the α/β boundaries in the β phase upon the growth of the α phase (Fig.6b). The concentration gradient ($C_{\beta}^{\beta/\alpha} - C_0$) in the β phase is also considered as a driving force of the α phase growth in the alloy.

2.3 Dilatometry curve analysis and CCT diagram building

The dilatometry curve of the Ti-1300 alloy cooled at 0.3 °C/s is shown in Fig. 7. A small variation in the dilatometry curve was observed upon continuous cooling from 850 °C to room temperature at a rate of 0.3 °C/s. This finding is attributed to the small variation in volume of the $\beta \rightarrow \alpha + \beta$ transformation under continuous cooling[29]. However, obvious variation was found in the derivative curve of the dilatometry curve vs. temperature under continuous cooling. This variation is related to α phase precipitation occurring within the β matrix upon continuous cooling at 0.3 °C/s. The precipitation of α phase indicates a specific volume

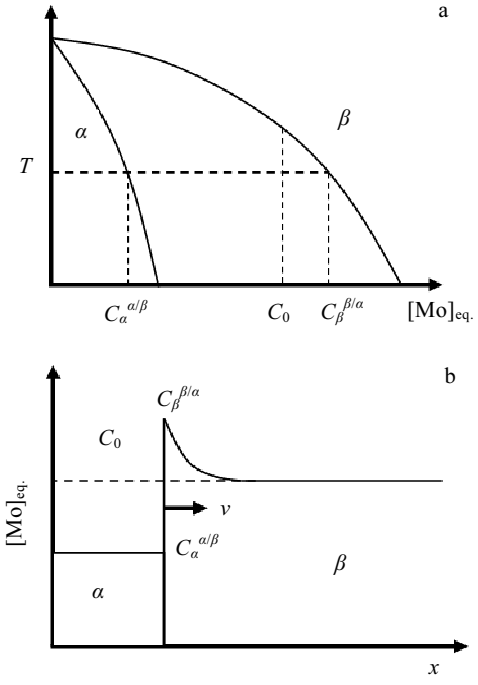

Fig.6 Distribution diagrammatic sketch of β stabilizing elements during growth process of α phase in Ti-1300 alloy

variation, which consequently makes the volume vary. Thus, the starting (T_s) and finishing (T_f) temperatures of the $\beta \rightarrow \alpha + \beta$ transformation, which were 613 and 457 °C, respectively, could be determined in the Ti-1300 alloy continuously cooled at 0.3 °C/s. We concluded that the $\beta \rightarrow \alpha + \beta$ transformation, at a cooling rate of 0.3 °C/s, occurred in a temperature range from 613 °C to 457 °C. Using the same method, the starting and finishing temperatures of the $\beta \rightarrow \alpha + \beta$ transformation could also be determined in the alloy cooled at various rates. Moreover, the critical cooling rate, which is around 3 °C/s, could be determined under continuous cooling in the alloy.

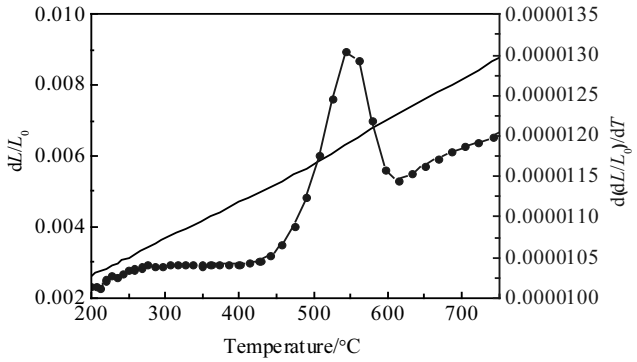

Fig.7 Dilatometry curve of Ti-1300 alloy cooled at 0.3 °C/s

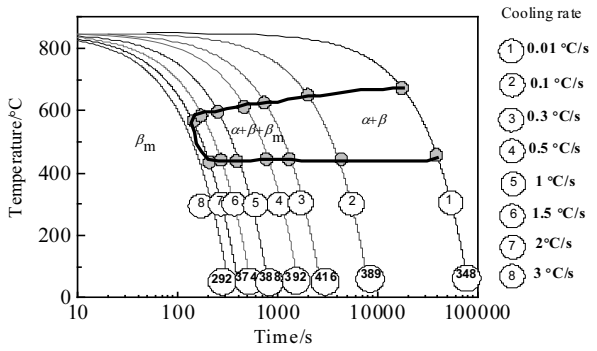

Fig.8 Continuous cooling transformation (CCT) curves of Ti-1300 alloy

The characteristic temperatures for the $\beta \rightarrow \alpha + \beta$ transformation were plotted in a CCT curve of the Ti-1300 alloy. As shown in Fig.8, the CCT curve illustrates the temperature and time variations required for phase transformation in the alloy at different cooling rates. Moreover, the time-axis is logarithmically scaled. Starting and finishing temperatures of the $\beta \rightarrow \alpha + \beta$ transformation in the Ti-1300 alloys at the each cooling rate are marked at corresponding cooling curves and connected by a smooth curve. The critical cooling rate is also marked in the CCT diagram of the Ti-1300 alloy.

As shown in Fig. 8, the precipitation of the α phase takes place mainly in the intermediate temperature region. The microstructure, which consists of α and β phases, could be obtained at a cooling rate slower than 0.1 °C/s. However, a retained metastable β phase is found in the microstructure of the Ti-1300 alloy at a cooling rate higher than 0.3 °C/s because it contained many stabilizer elements. Nevertheless, the volume fraction of the retained metastable β phase can reach 100% in the alloy at cooling rates that are higher than critical cooling rate of 3 °C/s. The critical cooling rate is remarkably sensitive to the chemical components of an alloy. The critical cooling rate of Ti-B19 is 0.3 °C/s, which was tested by Chang using electrical resistivity measurements [30]. Nonetheless, the critical cooling rate of β-CEZ is 10 °C/s [8], mainly because the molybdenum equivalents of Ti-1300, Ti-B19, and β-CEZ are 12.8, 15, and 5.1, respectively.

Fig. 8 shows the variation of micro-hardness in the alloys at various cooling rates. The micro-hardness of the alloys initially increased and then decreased with increasing cooling rates under continuous cooling conditions. The profound effects of microstructure on the mechanical properties of metallic materials are well-known. The Ti-1300 alloys consist of a lamellar $\alpha + \beta$ microstructure at a cooling rate slower than 0.1 °C/s. At this time, given that the cooling rate is slower, the final microstructure of the alloys becomes coarser. Thus, the volume fraction of the α/β phase boundaries increased with decreasing cooling rates. Phase boundaries are generally known to be particularly effective obstacles to dislocation motion, because crystallographic factors do not permit the passage of a dislocation from one phase to an adjacent one through a phase boundary[31]. Therefore, the micro-hardness is higher in the alloys cooled at a rate of 0.1 °C/s than in the alloys cooled at a rate of 0.01 °C/s. However, the retained β phase occurred when the alloys were cooled at a rate faster than 0.3 °C/s, which led to decrease in the micro-hardness of the alloys.

3 Conclusions

1) The $\beta \rightarrow \alpha + \beta$ transformation of the Ti-1300 alloys is a typical diffusion solid phase transformation under continuous cooling when the cooling rate is slower than the critical cooling rate. At slower continuous cooling, platelet-like $\alpha + \beta$ structures are obtained. Moreover, the thickness of the platelet-like $\alpha + \beta$ structures decreases with increasing cooling rates. The metastable retained β phase appears at cooling rates higher than 0.3 °C/s.

2) The volume fraction of the metastable retained β phase increases with increasing cooling rates. The volume fraction of the retained metastable β phase can reach 100% in the alloy at cooling rates that are higher than critical cooling rate of 3 °C/s. The α precipitations with different orientation initially start to nucleate at prior β/β grain boundaries when Ti-1300 alloys are continuously cooled at 0.1 °C/s.

3) The morphology of α phase gradually evolves from globular to needle-like in the alloys with decreasing temperature, while the volume of the α phase increases.

4) The concentration gradient ($C_{\beta}^{\beta/\alpha}$-C_0) is considered as a driving force of the α phase growth in the alloy. The hardness of Ti-1300 alloys initially increase and then rapidly decreases with increasing of the cooling rate under continuous cooling.

References

1 Ivasishin O M, Markovsky P E, Semiatin S L. *Materials Science and Engineering A*[J], 2005, 405: 296
2 Boyer R R. *Materials Science and Engineering A*[J], 1996, 213: 103
3 Leyens C, Peters M. *Titanium and Titanium Alloys*[M]. Weinheim: WILEY-VCH Verlag GmbH &Co KGaA, 2003: 37
4 Karasevskaya O P, Ivasishin O M, Semiatin S L *et al*. *Materials Science and Engineering A*[J], 2003, 354: 121
5 Ivasishin O M, Markovsky P E, Matviychuk Y V *et al*. *Journal of Alloys and Compound*[J], 1996, 457: 296
6 Boyer R R, Briggs R D. *Journal of Materials Engineering and Performance*[J], 2005, 14: 681
7 Behera M, Mythili R, Raju S *et al*. *Journal of Alloys and Compound* [J], 2013, 553: 59
8 Angelier C, Bein S, Bechet J. *Metallurgical and Materials Transactions A*[J], 1997, 28: 2467
9 Malinov S, Guo Z, Sha W *et al*. *Metallurgical and Materials Transactions A*[J], 2001, 32: 879
10 Kim S K, Park J K. *Metallurgical and Materials Transactions A* [J], 2002, 33: 1051
11 Fei Y, Zhou L, Qu H *et al*. *Materials Science and Engineering A*[J], 2008, 494: 166
12 Zhou Z, Lai M, Tang B *et al*. *Materials Science and Engineering A*[J], 2010, 527: 5100
13 Shah A K, Kulkarni G J, Gopinathan V *et al*. *Scripta Metallurgical Materialia*[J], 1994, 32(9): 1353
14 Briki J, Ben Slima S. *Journal of Materials Engineering and Performance*[J], 2008, 17: 864
15 Liu Y C, Sommer F, Mittemeijer E J. *Acta Materials*[J], 2003, 51: 507
16 Sun F, Li J, Kou H *et al*. *Journal of Alloys and Compound*[J], 2013, 576: 108
17 Tarín P, Alonso I, Simón A G *et al*. *Materials Science and Engineering A*[J], 2008, 481-482: 559
18 Zhao Y Q, Ge P, Qu H L. *Chinese Patent*[P], 200510000974.0. 2005
19 Zhao Y Q, Hong Q, Ge P. *Metallograph of Titanium and Titanium Alloys*[M]. Changsha: Central South University Press, 2011:125 (in Chinese)
20 Zhao Y H, Ge P, Zhao Y Q *et al*. *Rare Metal Materials and Engineering*[J], 2009, 38: 46 (in Chinese)
21 Zhao Y H, Ge P, Yang G J *et al*. *Rare Metal Materials and Engineering* [J], 2009, 38: 550 (in Chinese)
22 Wan M P, Zhao Y Q, Zeng W D *et al*. *Journal of Alloys and Compound*[J], 2015, 619: 383
23 Wen J H, Ge P, Yang G J *et al*. *Rare Metal Materials and Engineering*[J], 2009, 38: 1490 (in Chinese)
24 Wan M P, Zhao Y Q, Zeng W D. *Rare Metals*[J], 2015, 34(4): 233
25 Lu J W, Zhao Y Q, Ge P *et al*. *Materials Science and Engineering A*[J], 2015, 621: 182
26 William D, Callister J. *Fundamentals of Materials Science and Engineering*[M]. New York: John Wiley & Sons, INC, 2001: 321
27 Salib M, Teixeira J, Germain L *et al*. *Acta Materials*[J], 2013, 61: 3758
28 Wyatt Z, Ankem S. *Journal of Materials Science*[J], 2010, 45(18): 5022
29 Sadovskii V D, Bogachev T N, Smirnov L V. *Fizika Metallov i Metallovedenie*[J], 1960, 10(3): 397
30 Chang H. *Solid Phase Transformation Kinetics and Microstructure Evolutions of Ti-B19 Alloy*[D]. Xi'an: Northwestern Polytechnical University Press, 2006: 103
31 Zhou H Q, Huang M Z. *Strength Theory of Metals*[M]. Beijing: Science Press, 1989: 78

连续冷却条件下 Ti-1300 合金的组织演变与连续转变图

万明攀[1]，温　鑫[1]，马　瑞[1]，赵永庆[2]

(1. 贵州大学，贵州 贵阳 550025)

(2. 西北有色金属研究院，陕西 西安 710016)

摘　要：通过 OM、SEM、TEM 和 EBSD 研究了 Ti-1300 合金在连续冷却条件下组织演变规律和亚稳 β 相的分解形式，并采用高精度膨胀法建立了合金的连续冷却转变动力曲线。结果表明：当连续冷却速度比较缓慢时，Ti-1300 合金发生 $\beta \rightarrow \alpha + \beta$ 转变，并获得集束状的显微组织；而当冷却速度 0.3 °C/s＜v＜1.5 °C/s 时，Ti-1300 合金发生 $\beta \rightarrow \alpha + \beta + \beta_m$ 转变，并获得细针状的 $\alpha + \beta$ 组织和残余的 β_m 相；当冷却速度大于 3 °C/s 时，Ti-1300 合金基本获得全部 β 相，所以把 3 °C/s 认为是合金的临界冷却转变速度。在缓慢冷却过程中，Mo 当量梯度是合金中 α 相生长主要动力。随着冷却速度的增加，Ti-1300 合金的显微硬度先增加后降低，在冷却速度为 0.3 °C/s 时，显微硬度达到最大值。

关键词：Ti-1300合金；组织演化；转变图；连续冷却；显微硬度

作者简介：万明攀，男，1982 年生，博士，副教授，贵州大学材料与冶金学院，贵州 贵阳 550025，电话：0851-83627683，E-mail: mpwan@gzu.edu.cn